JOURNAL OF MATERIALS SCIENCE **38** (2003) 4439–4449

Combinatorial characterization of polymer adhesion

A. J. CROSBY
Department of Polymer Science and Engineering, University of Massachusetts, Amherst, USA
E-mail: crosby@mail.pse.umass.edu

Based on the experience of the pharmaceutical industry, a new trend in research which relies upon combinatorial methodologies is being used to characterize the complexities of polymer adhesion. In this article, we begin the discussion with a brief background description of conventional techniques that are used for characterizing polymer interfaces. This background description not only highlights the key quantities that are used to describe interfacial strength, but it also demonstrates the challenges of developing high-throughput screening methods for this field. Next, we introduce three novel methods that use combinatorial design to increase the throughput in knowledge discovery for polymer adhesion. This introduction discusses the experimental protocol as well as the main features of analysis and informatics for these techniques.

1. Introduction

Polymer interfaces play an important role in numerous technologies ranging from biomedical implants to integrated circuit chips. Interfaces control conductivity, provide environmental protection, define mechanical strength, and ensure the overall reliability of a technological package. All of these roles rely upon the strength of the polymer interface. For example, conductivity cannot be controlled if the interfacial bond is broken. A tissue scaffold will not be successful unless a strong interfacial attachment is established. A cardboard box will be useless if tape cannot provide a strong interface. In general, these examples demonstrate that the ability of an interface to play its role is dependent upon our ability to properly engineer the adhesion, or interfacial strength.

Although many materials exist for controlling interfacial properties, we currently do not have the knowledge to "dial-in" interfacial properties by systematically controlling molecular architecture. This knowledge is critical for pushing the envelope in developing technologies such as nanotechnology and biomaterials where interfacial properties can and will play a significant role. Over the last several decades, progress has been made in our understanding of how polymer interfaces form and fail. We know that the strength of the polymer interface depends on several parameters including, but not limited to, surface chemistry, molecular architecture, geometry, strain history, and the environment. Although this understanding signifies progress, taking our understanding to the next level requires the daunting task of developing a knowledge base for how these parameters couple to define adhesion and building predictive models for the development of interfacial strength.

As in the pharmaceutical industry, the number of combinations of these different controlling parameters presents a significant challenge for industrial and academic researchers. Based on the experience of the pharmaceutical industry, a new trend in research which relies upon combinatorial methodologies is being used to facilitate our understanding of the complexities of polymer adhesion [1–4]. In this chapter, we begin our discussion with a brief background description of conventional techniques that are used for characterizing polymer interfaces. This background description not only highlights the key quantities that are used to describe interfacial strength, but it also demonstrates the challenges of developing high-throughput screening methods for this field. Next, we introduce three novel methods that use combinatorial design to increase the throughput in knowledge discovery for polymer adhesion. This introduction discusses the experimental protocol as well as the main features of analysis and informatics for these techniques. In the last section, we summarize the key points. This discussion is not intended to provide solutions for all challenges in polymer adhesion characterization, but its goal is to highlight the way of thinking that can increase the efficiency of knowledge discovery in a complex and important area of polymer science.

2. Conventional techniques

Several conventional methods are used to quantify the performance of polymer interfaces. A few of the more common characterization methods include the peel test, loop tack test, probe-type tests, lap shear, free-edge peel, and double cantilever beam experiments [5–7]. Each of these experimental methods is focused on a

particular level of adhesion or type of polymer. For example, peel tests, loop tack methods, and probe-type experiments are primarily used to quantify the adhesion of soft adhesives with varying degrees of adhesion. A common class of adhesives tested with these techniques is pressure-sensitive adhesives. Free-edge peel tests focus on the bonding of thin, glassy or semi-crystalline polymers. These coatings often find application in the electronics industry. Double-cantilever beam experiments and probe-type tests are conventionally used to quantify the adhesion of glassy polymers and epoxies that are used in a variety of application industries. Of these various techniques, we will specifically discuss two of them: the peel and probe-type tests. The aim of this discussion is to highlight the primary parameters that are controlled and recorded during typical adhesion tests, as well as the advantages and challenges of conventional adhesion testing methods.

2.1. Peel tests

One of the most common and accepted techniques for measuring polymer adhesion is the peel test [8–11]. In its simplest form, this test involves casting a polymer film on a substrate, which is typically rigid. The film for this test has a uniform thickness, or a backing material, that is capable of providing mechanical stability for subsequent peeling. After casting and drying the film, one edge of the film is gripped by a mechanical pulling device and subsequently peeled away from the substrate at a constant crosshead velocity and constant peel angle. During this peeling action, the velocity is recorded as well as the force that is required to peel the film from the substrate. For the most quantitative results, the entire force history should be recorded during the peel test. This force history acts as a "fingerprint" for the adhesion of the interface between the polymer film and the underlying substrate.

In analyzing the results of this test, several approaches are practiced. The simplest analysis involves recording the maximum force applied during the peel test and comparing the measurement to peak peel forces for other films. The key points to remember with this approach is that the force must be normalized by the width of the polymer film since wider films of equivalent composition require more force than narrower films, and the peak force may be non-representative of the interfacial strength along the length of a given interface. For the latter reason, many researchers prefer to record the average "steady-state" peel force during the peeling process and normalize this quantity by the film width [11]. Alternatively, the total energy of peel can be determined by integrating the area under the curve of peel force versus applied displacement. This total energy is normalized by the original area of the polymer interface (width $\times$ length). Both of these approaches (i.e., the normalized "steady-state" peel force and the normalized peel energy) provide statistically reliable data from which comparisons can be made.

At the heart of this measurement, as well as all adhesion tests, is the determination of the driving force for interfacial failure. Typically, the failure of an interface is considered analogous to a fracture process, similar to a crack in a bulk material. Accordingly, the driving force for fracture is the energy release rate, or $\mathcal{G}$, for which a crack tip advances [7, 9, 12, 13]. The units of the energy release rate are energy per unit area, or in SI units: J/m^2. For the peel test, the normalized "steady-state" peel and normalized peel energy are conventionally referred to as the energy release rate. For some material systems, this equivalence is true, but in many cases the stress distribution near the advancing peel front greatly complicates the distribution of applied force, and the overall force recorded during peeling does not truly represent the driving force for fracture. Consequently, the interpretation of the peel energy is complicated, and this quantity does not provide an absolute means of relating interfacial strength to the molecular structure of the interface for all systems. In peel tests, the measured quantities will depend upon the peel angle, peel velocity, backing material (if used), and the process of forming the interface. For relative comparisons, keeping these parameters as consistent as possible provides the best results. It should be noted that if a true energy release rate is quantified, the velocity effects can be related to the viscoelastic properties of the polymer film through a WLF relation [13].

2.2. Probe tests

To remove some of the complicating factors of the peel test, probe-type tests are often used as an alternative or complementary method [6, 14, 15]. For this discussion, the probe-type test will be described in the context of measuring soft adhesives, such as pressure-sensitive adhesives, although they also are used for glassy polymers and epoxies. In a probe-type test, a probe is brought into contact and subsequently separated from a flat layer at a constant crosshead displacement rate. Either the probe or the flat layer is cast from the polymer of interest and the other component is made from the complementary material of interest (Fig. 1). For the simplicity, let us consider a rigid probe and a flat, compliant polymer layer. The geometry of the probe can be either spherical or flat. A comparison of both geometries is beyond the focus of this chapter, but previous research has addressed these differences [16].

As the probe contacts and separates from the polymer layer, the applied displacement, resulting force, and if possible, the resulting contact area are recorded throughout the test. Similar to the peel test, the force versus displacement curve can serve as a "fingerprint"

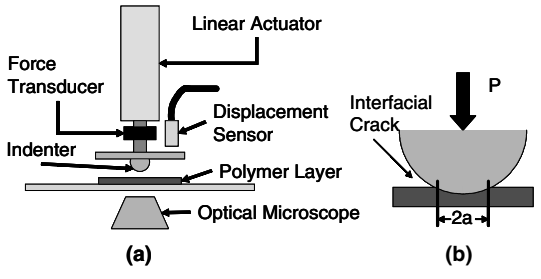

Figure 1 (a) Schematic of typical instrument used in probe-type characterization. (b) Definition of contact radius, a, as a force, P, is applied to a spherical indenter.

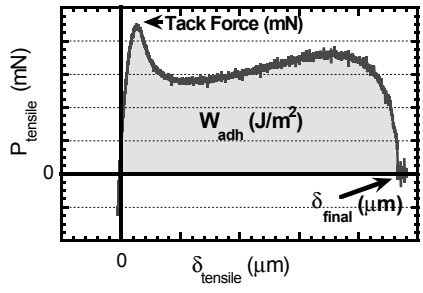

Figure 2 Typical force versus displacement results for a probe-type test. Definitions of measurable quantities are illustrated.

for the established interface if experimental conditions remain constant for comparisons (Fig. 2) [17]. The specific analysis of this test can also take many forms, as in the peel test. For qualitative comparisons, the simplest analysis is the comparison of the maximum tensile force from one polymer to another polymer. This maximum tensile force is often referred to as the "tack" force and should be normalized by the maximum contact area. This analysis is not consistently representative of the interfacial strength and can be greatly influenced by numerous uncontrollable parameters. Another useful quantity for comparative studies is the total energy for interfacial failure, or the area under the force-displacement curve. The total energy is normalized by the maximum contact area and is referred to as W_{adh}. Although W_{adh} has units of energy per unit area, it is not necessarily the energy release rate, or driving force for interfacial fracture. W_{adh} is a combination of the energy being used to create new surfaces through interfacial failure as well as the energy being dissipated in the bulk of the polymer film [18]. This balance of interfacial and bulk contributions to adhesion is a distinguishing ratio that marks the differences in adhesion across the variety of polymer interfaces. Consequently, decoupling and quantifying these contributions allows us to relate the molecular properties to the overall adhesion. As in the peel test, significant progress has been made in decoupling these contributions by properly quantifying the driving force for interfacial failure, $\mathcal{G}$ [13, 15, 19–21].

To determine $\mathcal{G}$, the energy release rate, for probe-type tests, a relationship based on the combination of contact mechanics and fracture mechanics is used. This relationship is often referred to as the JKR theory although alternative forms and modifications have been introduced over the last several decades [12, 15, 22]. To use this relationship, the contact area must be measured during the experiment. The contact area provides critical information not only for the fracture mechanics analysis, but also for many qualitative comparisons that are made using probe-type experiments. In a classical measurement, the fracture analysis depends upon the applied force, the resulting contact area, and the material's mechanical properties. Based on a balance of interfacial and elastic restoring forces, the following relationship is found [15]:

$$\mathcal{G} = \frac{3(P' - P)^2}{32\pi E a^3} \tag{1}$$

where $\mathcal{G}$ is the energy release rate, E is the elastic modulus of the system, R is the radius of curvature of the probe, P is the applied force, a is the radius of the contact area. P' is the required force to establish a contact radius of a in the absence of adhesion. P' is a derived quantity that is directly related to the Hertzian contact mechanics relationships established in the late 1800's [23]. The relationship in Equation 1 is only valid for elastic materials in an unconfined state. Although recent modifications do allow confined and linear viscoelastic materials to be quantified, the details of these modifications are beyond the focus of this chapter [15]. For our purposes, the most important point is that a probe-type test can provide the necessary information for determining the driving force for interfacial fracture. This driving force, if properly quantified, is a parameter that can be used to quantify interfacial strength independent of experimental conditions. This independence marks a quantity that can potentially be linked to the molecular interfacial interactions.

Although this analysis can provide a measurement of interfacial strength for many polymer systems, it is rarely used in industrial laboratories due to its complexity and the lack of contact area information in many probe-type test investigations. For this reason, a recent research effort focuses on the development of high-throughput adhesion characterization methods. These methods, as highlighted in the following sections, provide multiple advantages. First, the methods can be used as a screening mechanism to discover knowledge in a short amount of time. This increase in efficiency provides more time for further analysis on the systems and conditions that yield promising results. Second, many of the techniques provide both qualitative and quantitative data. A quick qualitative analysis can be used for screening, while quantitative data can be obtained if further detail is required. These two levels of analysis let the user optimize the balance of throughput and knowledge discovery. Finally, many of these measurements introduce methods for including calibrated standards within the libraries. These standards are exposed to the same processing and environmental conditions as the other variable sections, thus minimizing sources of statistical error that are typically introduced in conventional testing.

3. Combinatorial characterization methods

In this chapter, we introduce three techniques that have been developed recently to provide high-throughput, combinatorial measurements of polymer adhesion. These three methods are the multilens contact adhesion test (MCAT), the combinatorial edge delamination test, and the combinatorial peel test. As with conventional characterization methods, each technique focuses on a particular level and type of polymer adhesion. Although we discuss the technical procedures and analysis of these techniques, the thought process in developing and implementing these techniques is the common link. Combinatorial methodologies are truly a way of thinking, and the methodologies outlined in this chapter exemplify the thought process of combinatorial materials science.

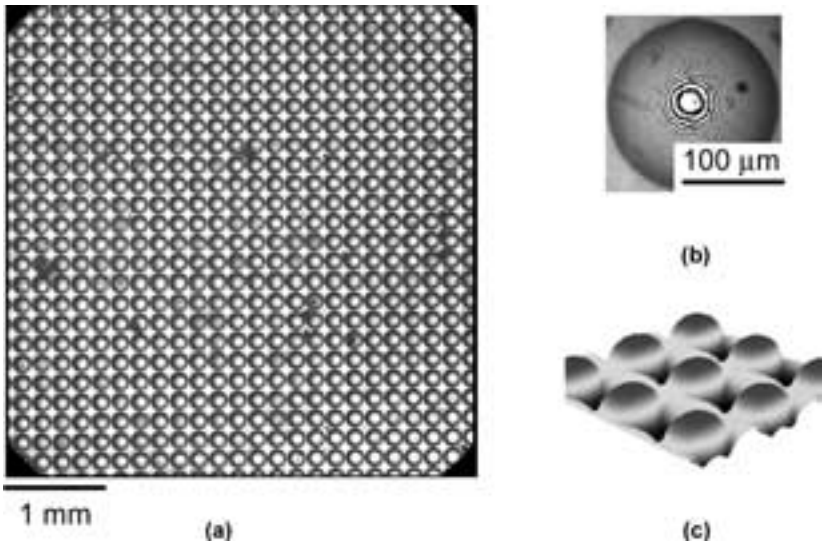

Figure 3 (a) Array of microlenses fabricated from polydimethylsiloxane. (b) A single microlens. The interference rings can serve as high-resolution displacement sensors for sensitive measurements. (c) Surface topography map of microlens array subset.

3.1. Multilens contact adhesion tests (MCAT)

The multilens contact adhesion test (MCAT) is largely based on probe-type tests [4, 24]. In this combinatorial experiment, an array of probes, such as spherical caps, is fabricated on a single substrate (Fig. 3). This array is brought into contact with a flat complementary substrate, and the two components are subsequently separated as in a conventional probe test. During the process of contact and separation, automated optical microscopy is used to track the changes in the contact area for each probe while the relative displacement of the overall array is recorded. With these two measurable quantities (i.e., contact area and displacement), the adhesion of the interface at each point of contact can be qualitatively and quantitatively evaluated. By using combinatorial library fabrication methods that are known to the field of combinatorial materials science, every point within the contacting array can potentially quantify the adhesion of a unique combination of adhesion-related parameters. In existing libraries, this increase in throughput can translate into upwards of 8000 adhesion experiments being conducted in the equivalent time of one conventional adhesion experiment.

To discuss the details of this technique, as well as the advantages and challenges associated with it, we delineate the four steps involved in the procedure: library design, library fabrication, library evaluation, library analysis.

3.1.1. MCAT library design

The library in a MCAT experiment consists of two components: the array of spherical caps and the complementary flat substrate. Library design for MCAT experiments is concerned with three main factors: materials selection, geometry of the lens array, and definition of the parameter space that will be investigated.

For material selection, either the array probe or the complementary substrate can be fabricated from the polymer of interest and either can be rigid or solid. For the convenient analysis, it is recommended that one component be rigid and one be more compliant. Most importantly, in choosing the respective material assignments, the researcher decides from which material a lens array will be most easily fabricated. Although each component has individual considerations, the only rule that must be applied to the overall library system is that at least one of the components must be optically transparent. The MCAT methodology relies upon contact area data and the relative displacement of the array. If the contact areas cannot be recorded, the MCAT methodology will not work efficiently.

The geometry of the lens array consists of three primary dimensions: the lens radius of curvature, the interlens spacing, and the overall size of the array. The radius of curvature is determined by the contact area that will be established and the thickness of the compliant component. To minimize confinement effects (which require correction factors for a quantitative analysis), the maximum contact radius established during a test should be no greater than one fifth of the radius of curvature and one half of the thickness of the compliant component. These rules are recommendations for simplifying the analysis. The radius of curvature also should be chosen to sample the proper area that represents a state point in the combinatorial library. To define state points in a combinatorial library, refer to Meredith *et al*. [3].

Related to the definition of a state point is the design of the parameter space that will be investigated. As mentioned above, the fabrication of combinatorial libraries in polymer science has been a focus of recent research. Many of the parameters that can be controlled in a combinatorial manner affect adhesion. A few of these parameters include temperature, composition, surface energy, and thickness [3, 25, 26]. In designing the parameter space for a MCAT experiment, consider parameters that can be effectively varied across the extents of the overall library. Also remember that each lens does not need to probe a unique point in parameter space. If multiple contacts are made within a state point, then

these increased statistics can enhance the reliability of the measurement.

The interlens spacing, L, is a critical design parameter since it dictates the mechanical and adhesive coupling between contact points. To prevent the coupling of lenses, the maximum contact area should be much less than the interlens spacing. For the case of cylindrical features on a surface, Hui *et al.* have used theoretical arguments to suggest that the L should be [27]:

$$L \geq \left(\frac{32\pi w R^2}{0.57E} \right) \tag{2}$$

to avoid spontaneous interlens coupling. In this equation, w is the work of adhesion, R is the radius of curvature, and E is the effective modulus for the contacting system.

The last dimension to consider in designing the library is the overall dimensions of the lens array. This dimension is dependent upon the maximum range of travel in the automated microscope stage and the maximum force range of the actuators that drive the two library components into contact. The total applied force is directly related to the total contact area (i.e., the sum of the contact areas for all individual lenses). Therefore, the total applied force should not exceed the specifications of the actuators, nor should the total array size be larger than the range of travel for the microscope stage.

3.1.2. MCAT library fabrication

After designing the MCAT library, the next step involves fabricating the libraries. Numerous methods exist to construct the lens arrays, but the details greatly depend upon the materials and size scale that are chosen in the design step. If large lenses from a soft material are required, conventional techniques used in the fabrication of JKR-type lenses can be utilized [28, 29]. If large lenses from a rigid material are required, many suppliers fabricate rigid spherical caps for the optics industry. In this case, the individual lenses can be arranged manually into a two dimensional array, fixed, and used. In many cases, proper cleaning and storage of a lens array can allow lenses to be used repeatedly. If the lens arrays are required to be small and compact, numerous parallel, self-assembly techniques have been described in the literature for making microlens arrays. These techniques or the method for making elastomeric stamps typically used in soft-lithography processing can be used [24, 30–35]. An example of microlens array that was fabricated using steps similar to those in soft-lithography processing is shown in Fig. 3. The main objective in the fabrication of the lens arrays is to use a method that allows the shape and composition of the individual lenses to be controlled and uniform. Uniform lenses on a planar substrate simplify the analysis of the MCAT results, thus increasing the throughput and knowledge discovery.

For the complementary substrate, any material can be used. The rigid material for the complementary substrate can be either the material of interest or it can simply act as a supporting layer for other materials that will be used in the combinatorial investigation. For example, in many recent MCAT experiments, silicon wafers and glass microscope slides have been used as complementary substrates. In these cases, the rigid substrate has been coated using conventional or combinatorial techniques. An example of a conventional technique is spin-coating or doctor blading. A combinatorial coating technique is flow coating which applies a polymer coating with a continuous thickness gradient in one direction. As in the fabrication of the lens arrays, any technique or material can be adopted for the complementary substrates. The most important point is to meet the criteria of the library design. For example, if small microlens arrays have been chosen for the investigation, the roughness of the complementary substrate should not be commensurate with the size scale of the microlenses. This combination will result in nonuniform contact areas that complicate a parallel analysis routine.

3.1.3. MCAT library evaluation

The evaluation step in a combinatorial methodology involves conducting the experiment. For the MCAT technique, the experiment consists of the two dimensional array of lenses contacting and separating from the complementary substrate. To conduct this test, the appropriate instrument and steps must be used.

The MCAT instrument is designed to perform essential tasks while satisfying the throughput requirements of the research laboratory. In other words, the tasks can be automated (providing the highest-throughput) or performed manually. First, the MCAT instrument drives the two libraries into contact and controls their subsequent separation. A manner for accomplishing this task is to fix one component to a stationary base and use a linear actuator (automated or manually-driven) to move the other component into and out of contact. Prior to contact and separation, the two components are aligned. Since the lens array and the complementary substrate are planar objects, to properly map the adhesion of the entire library, the entire microlens array should contact the complementary substrate. Although each lens is not required to contact the substrate at the same time, the two components should be sufficiently aligned to permit contact over the entire array. Alignment can be achieved by having one component fixed to a tip/tilt stage that can be adjusted with precision for the given length scales associated with the library design.

After alignment and during the process of contact and separation, the collection of data is completed throughout the history of the test. The primary parameters that are recorded are the contact areas of each lens and the relative displacement of the overall array. To quantify the relative displacement, optical displacement sensors and capacitance based sensors provide convenient and simple measurements. The key feature of these sensors is that the measurement is made without contacting either library component. Contact based displacement measurements can affect the force or displacement distribution applied to the lens array. Using an external displacement sensor rather than relying upon the internal encoder of the actuator also is advised since it limits the effect of instrument compliance in the accuracy of the adhesion measurement.

To record the contact areas, an optical microscope or video camera with appropriate objectives should be used to monitor the interface. If the entire array cannot be imaged in one field of view with sufficient resolution, an automated system of *x*-*y* translation stages permits the ordered mapping of a large sample through multiple image captures. This "automated" optical microscopy is a standard feature on many current optical microscopes or can be custom-built as described in Meredith *et al.* [25].

To conduct the experiment, two modes can be used. The first mode is a continuous-motion mode. In this scenario, the actuator drives the two components into and out of contact at a constant displacement rate. During the displacement of the components, the displacement and contact area measurements are recorded at a fixed rate. The time and spatial resolution of the displacement and contact area measurements should be sufficient to provide at minimum five data points upon contact and five data points upon separation. To synchronize the data in this mode, a time stamp should be used to correlate the contact area and displacement measurements. The advantage of this mode is that the velocity at which the contact area changes can be quantified for each lens. As found in previous research, the rate of change in the contact area dictates the interfacial properties of many polymer systems.

The alternative option for an MCAT experiment is a step-motion mode. Here, the actuator displaces an arbitrary step distance. After the step is completed, the system is allowed to equilibrate for an arbitrary time before proceeding to the recording of the displacement and contact areas. This equilibrium time allows the contact areas to stop changing at a given displacement, thus ensuring that the contact area and displacements across the array will be properly compared. The advantage of this mode is that time synchronization is not necessary for correlating the contact area and displacement data. This mode also is most adaptive to high-throughput analysis and mapping. The disadvantage of this mode is that velocity dependent properties are not captured and can lead to non-absolute measurements.

3.1.4. MCAT library analysis

Qualitative and quantitative approaches to analyzing MCAT experiments can provide rapid, high-throughput solutions to adhesion characterization. To qualitatively analyze the MCAT data, the most valuable approach is the visual observation of the overall array during contact and separation. This approach is demonstrated in Fig. 4. The MCAT library is designed to have the lenses with the greatest adhesion remain in contact the longest total time. In other words, if the two components of the MCAT library are well-aligned, then the region or lenses that separate last define the conditions where maximum adhesion is experienced. This qualitative analysis provides an efficient means of mapping the adhesion of a surface on a comparative level. In fact, for quality control screening in an online process this approach could be augmented by including a row or region of well-defined standard interfaces. These standard interfaces would act as a benchmark for visual comparisons of the adhesion of the other lenses in the library.

To analyze the MCAT results in a quantitative manner, the first task is to measure the contact areas of the individual lenses throughout the history of a given experiment. This task is best accomplished by using image processing software such as Image-Pro, NIH Image, or Scion Image. After the contact areas are measured, they are converted to contact radii, and correlated to the relative displacement for each lens. The time of the contact area image and the time of the displacement measurement serve as a convenient means of synchronization. Each lens has a unique definition of zero displacement where the relative displacement for a given lens is defined as zero at the initial point of contact. This definition provides a natural adjustment for minor misalignment between the two library components. As the contact radii and displacements are correlated, they should also be recorded with the array coordinates of the lens position. The spatial coordinates of the lens defines the conditions in parameter space under which the interface is formed and failed.

For each lens, the contact radius is plotted as a function of the applied relative displacement. The resulting curve is referred to as the contact history for a given lens (Fig. 5). This contact history is used to determine the three main quantities that are used to describe the adhesion of the interface at each point in the combinatorial library. The first quantity that is measured is the hysteresis. For an elastic system, the hysteresis of the contact history is related to the total dissipated energy during the failure of the interface. For viscoelastic systems, the relation is more convoluted, but qualitative comparisons can still be made with this quantity.

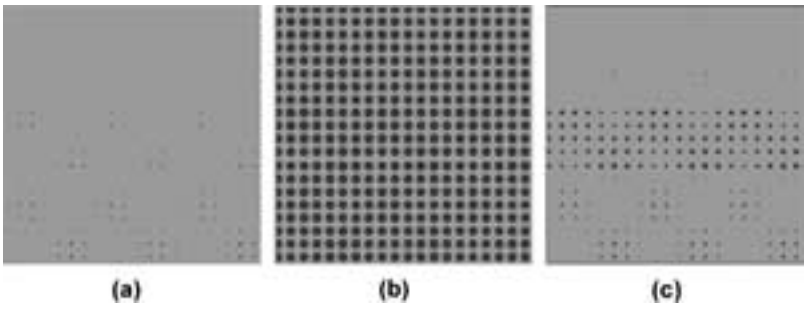

Figure 4 Sequence of images illustrating contact history of an MCAT experiment at three representative times: (a) approach, (b) maximum contact and (c) retraction. These results are a simulation where the center region of lenses have a higher adhesion, thus causing them to remain in contact the longest.

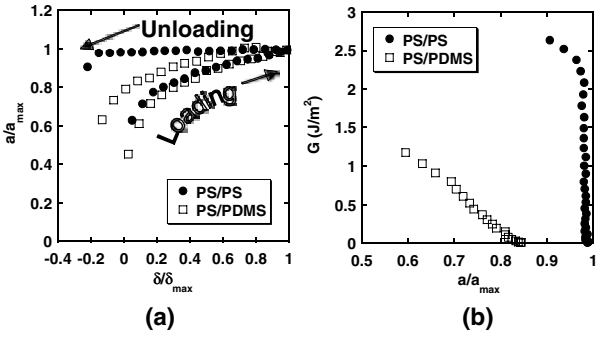

Figure 5 (a) Contact history for two lenses with different interfaces. The PS/PS interface exhibits significant hysteresis while the PS/PDMS interface exhibits no hysteresis. (b) Driving force for interfacial failure, $\mathcal{G}$, as a function of normalized contact radius for both interfaces. (Used with permission from Crosby *et al*. [24]).

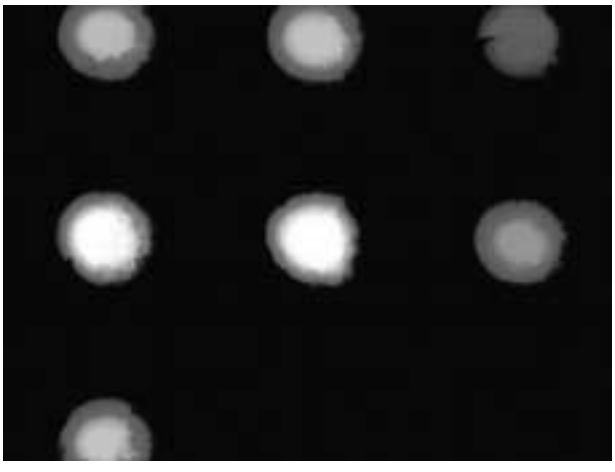

Figure 6 Contact history map of seven microlenses at a fixed displacement. Pixel intensity is directly related to time of contact (i.e., bright spots remain in contact the longest).

Another quantity that is easily determined from the contact history is the strain at final failure. These two quantities provide quick comparative quantities for making relative, quantitative measurements across the combinatorial library, but they do not constitute an absolute measurement of adhesion.

To quantify the interfacial strength, the driving force for interfacial fracture must be determined. For elastic systems, this driving force is typically referred to as the energy release rate, $\mathcal{G}$. For the combinatorial library in the MCAT experiment, $\mathcal{G}$ is calculated by rearranging Equation 1, and using $\mathcal{G}$ as fitting parameter for defining a curve to best-fit the contact history. For viscoelastic materials, a similar quantitative approach can be used, but the details are beyond the scope of this discussion. The driving force, $\mathcal{G}$ for elastic systems, is then plotted as a function of the normalized contact radius (Fig. 5b) or the interfacial crack velocity, da/dt. The critical energy release rate for propagating an interfacial crack is dependent upon the crack velocity, and this relationship has been shown to be an absolute property of the interfacial system [13, 18, 29].

Although producing contact history plots, calculating the final failure strain, and determining $\mathcal{G}$ vs. da/dt is a conventional means of analyzing a contact adhesion test, the knowledge discovery benefits of the MCAT are not augmented by these conventional means of analysis. To discover trends in the development of adhesion in multivariable environments, the results of an MCAT experiment are best presented in a new, adhesion-map format. An example of map format is the contact history map that is shown in Fig. 6. In this figure, an image sequence of 850 images (nearly one gigabyte of data) is collapsed into a single image. To accomplish this storage and presentation format, image processing software and custom-written routines are used to represent time of contact with pixel intensity/color. Through this transformation, the resulting image is a map where the lens remaining in contact the longest is indicated by the brightest pixels. In addition to contact time, similar maps can be created for $\mathcal{G}$, W_{adh}, and da/dt.

3.1.5. MCAT example

To demonstrate the MCAT process, we briefly describe an example that demonstrates the main concepts. This experiment was performed and reported by Crosby *et al.* in a recent publication [4, 24].

In this example, Crosby *et al.* used the MCAT methodology to compare the interfacial strength of polystyrene/polydimethylsiloxane (PS/PDMS) interfaces to polystyrene/polystyrene (PS/PS) interfaces. For the initial investigation, the library was designed to have two distinct regions: (1) PS/PS interfaces and (2) PS/PDMS interfaces. To fabricate this library, a microlens array was fabricated from crosslinked-PDMS. This PDMS microlens array was made by using a molding technique similar to the process for making stamps for soft-lithography. An image of the microlens array is shown in Fig. 3. To create the two regions in this library, the center region of the PDMS array was coated with a thin film of polystyrene. This coating was applied through a water-floating technique that has been described previously [24]. For the complementary substrate, a silicon wafer was spin-coated with a uniform thin film of polystyrene. This combination of partially-coated PDMS microlens array and PS-coated silicon wafer will create the designed library of two distinct interfacial composition regions upon contact.

After fabricating the library, the two components were placed on the MCAT instrument and subsequently brought into and out of contact in one continuous motion. Specifically, the silicon wafer was held in a fixed position while the microlens array was moved at a fixed displacement rate of 1 μm/s by a motorized linear actuator. An upright microscope was used to visually observe and record the contact areas across the library. For the first test, the library components were brought into contact at a fixed temperature of 25°C. At this temperature, the interfacial strength of the PS/PDMS and PS/PS regions were equivalent within the resolution of the MCAT instrument that was used. For the second test, the same library was brought into contact at an elevated temperature of 80°C. At this temperature, the polymers in the symmetric glassy polymer interface diffuse across the interface. This diffusion creates entanglements that strengthen the interface. For the quantitative analysis, the contact history for two individual lenses was measured manually (Fig. 5). This contact

history clearly shows the increase in hysteresis at the elevated temperature for the glassy polymer interface. Accordingly, from the contact history the energy release rate for the two interfaces at the elevated temperature can also be calculated (Fig. 5).

The increase in adhesion at the PS/PS interface is sufficient to fail the PS coating on the PDMS array. In other words, the applied energy required to propagate an interfacial crack at the newly formed PS/PS interface exceeds the required energy for propagating a crack through the PS coating on the PDMS array. This difference in fracture strength results in a "weld" spot being deposited onto the PS-coated silicon wafer. This welding does not occur in the test conducted at 25°C, but it occurs within the time of the test conducted at the elevated temperature of 80°C. This observation led Crosby *et al.* to quantify the critical temperature for welding of PS/PS interfaces.

To determine the critical welding temperature of PS/PS interfaces, Crosby *et al.* designed a combinatorial test to determine the influence of coating thickness on the critical welding temperature. The MCAT library for this test is similar to the one described above with the exception that the entire PDMS array is coated with a PS thickness gradient coating. This thickness gradient PS coating was applied to the PDMS microlens array through the same water-floating technique as in the previous study. The complementary substrate for this measurement was a PS-coated silicon wafer that was fixed to a temperature gradient stage. During the process of contact and separation, the two library components are arranged such that the thickness gradient is orthogonal to the applied temperature gradient. This design allows each contacting lens to measure a unique combination of temperature and thickness. The result of this measurement is shown in Fig. 7. Clearly, the critical welding temperature does depend on the thickness of the coating over a range of thicknesses. This trend of how coating failure depends on thickness and temperature is discovered within the same time required to conduct a single conventional adhesion measurement at one temperature and one thickness. In addition to the qualitative trend displayed in Fig. 6, the entire contact history from this experiment can be used to quantify the adhesion and fracture energies across this parameter space. The choice of analytical detail remains with the user.

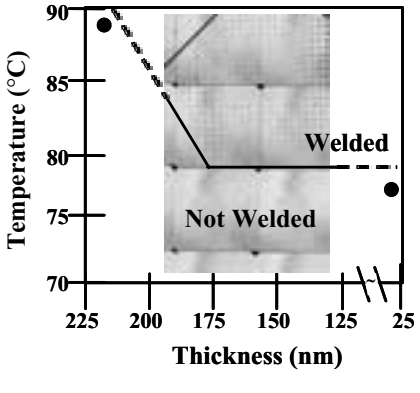

Figure 7 Results of MCAT experiment that measured the dependence of welding temperature for coating failure on coating thickness. Two individual data points were collected using uniform conditions. "Welded" region denotes coating failure. (Used with permission Crosby *et al.* [24]).

3.2. Combinatorial edge delamination tests

Edge delamination tests are commonly used in the electronic packaging industry to evaluate the adhesion/debonding of polymer coatings that are used as insulating or bonding layers. The conventional edge delamination test requires a rectangular coupon of a defined substrate material to be coated with a polymer film of interest. This coupon is placed in an oven at an elevated temperature, allowed to equilibrate thermally at this temperature, and subsequently quenched to a lower temperature. During the quenching process, the mismatch in the thermal expansion properties of the polymer film and the underlying substrate in conjunction with the natural stress-concentrating geometry at the coupon's corners causes interfacial failure to occur between the polymer coating and the substrate. The magnitude of the stress applied to the interface is a function of the mismatch in thermal expansion properties, the thickness of the polymer coating, the stiffness of the polymer coating and substrate, and the change in temperature incurred during the quenching process. Accordingly, by conducting several tests at different temperatures and thicknesses, a database can be collected to define a failure map of critical temperature and thickness combinations above which failure will be prevented. This information is especially helpful for design engineers in the electronic packaging industry where new materials must satisfy existing operating temperatures and pre-defined geometric constraints.

3.2.1. Free-edge library design and fabrication

Although the edge delamination test provides valuable results, the procedure of running numerous samples to define a single failure map is laborious, and uncontrolled errors can be introduced in the resulting map from sample to sample discrepancies. For these reasons, Chiang *et al.* conceptualized a simple, powerful technique to define failure maps for edge delamination tests by using combinatorial methodologies [36]. For this technique, the library consists of a single coupon with a polymer coating that has a thickness gradient in one direction. After applying the thickness gradient coating, the coating is divided into equally sized square regions. These square regions serve as individual delamination test samples fixed to a common substrate (Fig. 8). A temperature gradient for quenching the thickness gradient library is placed orthogonal to the thickness gradient. In this configuration, each square region probes the debonding strength of the polymer interface at four unique points in parameter space.

In this configuration, great care must be taken to ensure validity of the combinatorial evaluation. For example, if the library is not fabricated in the proper manner, the geometry of the library can cause one "free-edge" region to influence the debonding of a neighboring region. This "crosstalk" is the subject of the published

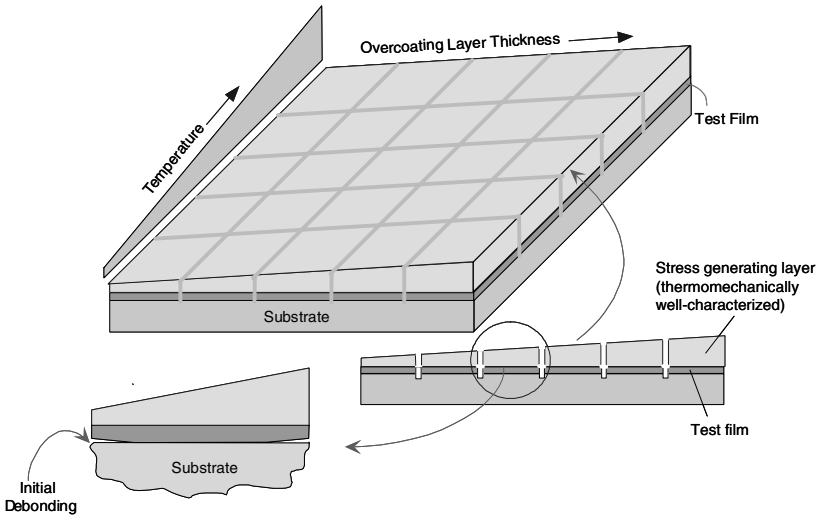

Figure 8 Schematic of combinatorial library for edge delamination characterization. (Used with permission Chiang *et al*. [36]).

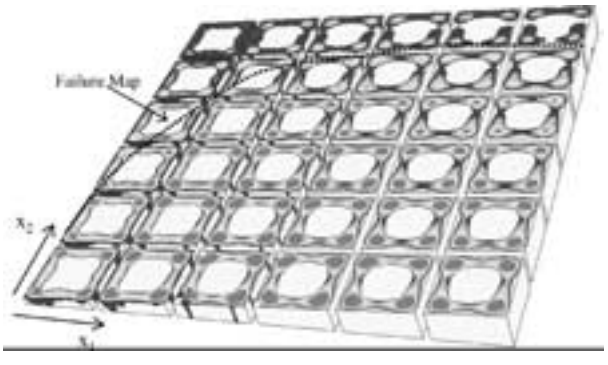

Figure 9 Finite element results of 6×6 edge delamination library. Failure map is defined by transition of bonded and debonded regions. (Used with permission from Chiang *et al*. [36]).

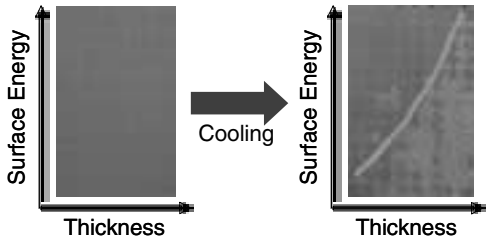

Figure 10 Edge delamination libraries before and after cooling. Line indicates failure map for critical surface energy at varying thicknesses, or related stresses. (Used with permission from Song *et al*. [37]).

work by Chiang *et al.* [36]. In this work, the researchers use finite element methods to establish standard guidelines to dictate the proper definition of combinatorial edge delamination test libraries. An example of the finite element results from this work is shown in Fig. 9. In addition to setting guidelines for proper library design, these finite element simulations also established the validity of the technique by producing a failure map for a well-characterized material.

3.2.2. Edge library evaluation and analysis

More recently, Song *et al.* have produced an experimental failure map for the adhesion of PMMA films on silicon substrates (Fig. 10) [37]. In these experiments, a PMMA film was fabricated with a thickness gradient ranging between 1 to 11 μm. Orthogonal to the thickness gradient Song *et al.* placed a surface energy gradient of the underlying substrate. This surface energy gradient was produced by depositing a self-assembled monolayer onto a silicon wafer surface. Upon exposing the methyl-terminated SAM layer to UV ozone, a variety of surface chemistries are created to alter the surface energy of the SAM surface. The dosage of the UV ozone is directly related to the relative change in surface energy [38], therefore, by controlling dosage in a linear fashion, a surface energy gradient was fabricated on the silicon wafer surface. The final library consisted of a PMMA film with a thickness gradient deposited on a SAM-coated silicon wafer with a surface energy gradient. This library was evaluated by exposing it to liquid nitrogen for 5 s. This low temperature quench created sufficient stress at the PMMA/SAM interface to initiate debonding in the regions of surface energy and thickness that develop the weakest interfaces.

3.3. Combinatorial peel debonding tests

3.3.1. Combinatorial peel design and evaluation

Similar to the combinatorial edge delamination test, Song *et al.* have developed a combinatorial peel debonding test [39]. The main difference between the two methods is that the stress used to initiate debonding is provided by the peeling of a pressure-sensitive adhesive rather than by thermal quenching. The library for this technique consists of a rigid substrate coated with a thin polymer film. This film is mechanically divided into discrete sections with a razor blade. The entire divided library is subsequently exposed to a gradient experimental parameter such as temperature or UV exposure. After this step, a pressure-sensitive adhesive is applied to the surface of the thin polymer film. This PSA serves as a carrier of an applied stress. The PSA is gripped by a mechanical testing instrument and peeled at a given angle from the underlying substrate. Consequently, in the regions where the adhesion of the thin

polymer film to the underlying substrate is greater than the adhesive strength of the PSA/polymer adhesion, the polymer film will remain on the underlying substrate. In the regions where the polymer/substrate adhesion is weaker than the PSA/polymer adhesion, the polymer debonds from the underlying substrate. Accordingly, this test can be used for a qualitative assessment of polymer film adhesion.

3.3.2. Combinatorial peel example

Song *et al.* used this technique to investigate the effect of surface energy and annealing conditions on the adhesion of PMMA thin films to rigid substrates [39]. Their motivation was to establish a high-throughput methodology to address the complex adhesion issues of photoresists and other polymer films used in the processing of microelectronic components.

For these experiments, a glass slide was coated with a self-assembled monolayer of *n*-octyl dimethylchlorosilane. This methyl-terminated SAM layer was subsequently exposed to a continuous gradient of UV ozone dosage. This gradient in dosage is created by using a line UV source that is positioned within 200 microns of the SAM surface. The SAM-coated substrate is accelerated under the UV source, thus exposing each region of the SAM layer to a decreasing dose of UV ozone. This process alters the surface chemistry of the SAM layer and creates a continuously changing surface energy on one substrate [38].

Onto this surface energy gradient, a PMMA film of uniform thickness was placed. The PMMA film was floated onto the substrate through a water-floating technique. This coating method was chosen to minimize spin-casting and solvent-evaporation effects on the adhesion of the PMMA/SAM interface since the evaporation of solvent can be analogous to annealing conditions for the PMMA film. After the water is allowed to evaporate from the sample, the film is divided into discrete strips with a razor blade. These strips extend along the surface energy gradient as shown in Fig. 11. This sample is then placed on a uniform temperature stage to anneal the PMMA film. At different times during the annealing, the sample is removed and a pressure-sensitive adhesive is applied to a single strip. This PSA film is gripped in a mechanical testing machine and the PMMA-coated substrate is held by the complementary grips in the machine. At a constant displacement rate,

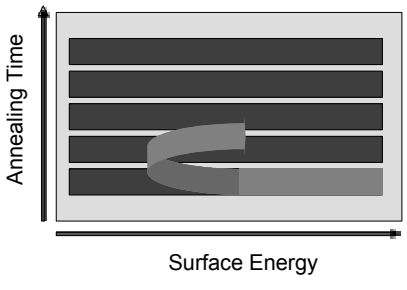

Figure 11 Schematic of combinatorial library design for peel delamination characterization of effect of annealing time and surface energy on the development of a PMMA/SAM interface.

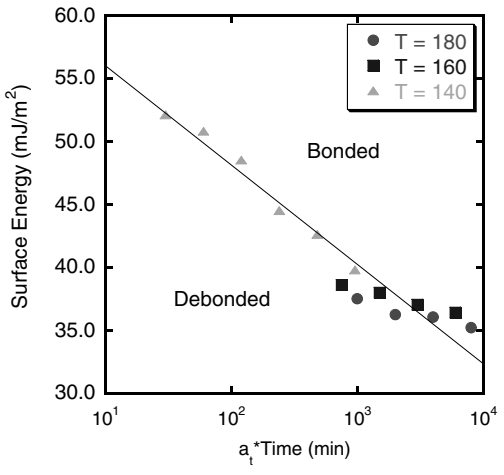

Figure 12 Failure map from combinatorial peel delamination test on PMMA/SAM interfaces. (Used with permission from Song *et al*. [39]).

the PSA film is peeled from the substrate at a 180 degree angle. During this peeling process, the PMMA film is debonded from the surface energy gradient. At a critical surface energy, the failure process no longer occurs at the PMMA/SAM interface, but it occurs at the PSA/PMMA interface. This change in failure mode defines the surface energy at which the driving force for interfacial failure of the PMMA/SAM interfaces equals or exceeds the driving force for interfacial failure of the PSA/PMMA interface. After peeling one strip, the remaining sample is placed on the temperature stage for additional annealing. This process is repeated until all strips have been tested. Upon completion, one library defines the development of the critical energy release rate, or fracture driving force, as a function of annealing time. Song *et al.* performed this experiment at three different annealing temperatures and demonstrated that the critical annealing times for different temperatures can be linearly shifted onto one curve in a manner analogous to the WLF shift factor (Fig. 12) [39].

This technique demonstrates how discrete samples and conventional testing methods can be combined with gradient and high-throughput methodologies to increase the efficiency of experimentation and knowledge discovery. Although the time axis is not a continuous gradient, Song *et al.* used a combinatorial approach by utilizing a single PMMA film, a single PSA tape, and a single modified-SAM substrate to create a library [39]. This technique minimizes the experimental variance that is associated with conventional testing methodologies while increasing throughput.

4. Summary

This chapter presents an overview of the recent developments in the use of combinatorial methodologies for characterizing polymer adhesion. Combinatorial methods are a way of thinking that can translate into all stages of experimental design. These methods not only increase the efficiency of discovering optimal formulations in the development of new adhesives, but they also increase the development of a knowledge database for reaching the broader, fundamental goals of the polymer adhesion community.

The initial discussion on conventional adhesion characterization methods serves as critical knowledge in the development and improvement of new combinatorial methodologies. This background allows us to make the connection between conventional techniques and combinatorial methods while understanding the compromises between screening parameter space and making quantitative measurements that relate to the molecular origins of adhesion. As in many combinatorial methods, the choice of analysis level remains with the user. This feature may play a strong role in the future exchange of data and understanding between industrial and academic research efforts since data can be collected and separately analyzed to meet the needs and time scales respectively.

The three methods highlighted in this chapter address the characterization of different polymer classes. These methods are currently used successfully, but the exploration of broader ranges of parameter space for all three techniques is ongoing. New methodologies and improvements of these existing techniques will undoubtedly be developed in the future. Accordingly, this chapter serves as a foundation for building of these future developments.

Acknowledgements

This work was supported by the National Institute of Standards and Technology, the NRC Research Associateship Program, and the Department of Polymer Science and Engineering at the University of Massachusetts at Amherst. The author gratefully acknowledges the advice and support of Dr. Eric J. Amis and Dr. Alamgir Karim, as well as the figures and helpful discussion provided by Dr. Martin Chiang and Dr. Rui Song.

References

1. B. JANDELEIT, D. J. SCHAEFER, T. S. POWERS, H. W. TURNER and W. H. WEINBERG, *Angew. Chem. Int. Ed.* **38** (1999) 2494.
2. E. W. McFARLAND and W. H. WEINBERG, *Trends in Biotech.* **17** (1999) Reviews.
3. J. C. MEREDITH, A. P. SMITH, A. KARIM and E. J. AMIS, *Macromolecules* **33** (2000) 9747.
4. A. J. CROSBY, A. KARIM and E. J. AMIS, *Abstr. Pap. Amer. Chem. Soc.* **222** (2001) 450.
5. D. A. DILLARD and Y.-H. LAI, *ANTEC* (1995) 2844.
6. C. CRETON, in "Materials Science and Technology: A Comprehensive Treatment," edited by R. W. Cahn, P. Haasen and E. J. Kramer (VCH Verlagsgesellschaft mbH, Weinheim, 1997) Vol. 18, p. 708.
7. J. G. WILLIAMS, "Fracture Mechanics of Polymers," 1st ed. (John Wiley & Sons: New York, 1984).
8. D. H. KAELBLE, *J. Coll. Sci.* **19** (1964) 413.
9. *Idem.*, *Trans. Soc. Rheol.* **9** (1965) 135.
10. *Idem.*, *J. Adhes.* **1** (1969) 102.
11. A. ZOSEL, *ibid.* **34** (1991) 201.
12. D. MAUGIS and M. BARQUINS, *J. Phys. D: Appl. Phys.* **11** (1978) 1989.
13. A. N. GENT and R. P. PETRICH, *Proc. Roy. Soc.* A. **310** (1969) 433.
14. H. R. BROWN, *Annu. Rev. Mater. Sci.* **21** (1991) 463.
15. K. R. SHULL, D. AHN, W.-L. CHEN, C. M. FLANIGAN and A. J. CROSBY, *Macromol. Chem. Phys.* **199** (1998) 489.
16. A. J. CROSBY, K. R. SHULL, H. LAKROUT and C. CRETON, *J. Appl. Phys.* **88** (2000) 2956.
17. H. K. CHUANG, C. CHIU and R. PANIAGUA, "Pressure Sensitive Tape Council Annual Technical Seminar" (Boston Park Plaza Hotel, 1997) p. 39.
18. A. J. CROSBY and K. R. SHULL, *J. Polym. Sci. Part B: Polym. Phys.* (1999) 37.
19. M. BARQUINS and D. MAUGIS, *J. Adhes.* **13** (1981) 53.
20. C. CRETON, J. HOOKER and K. R. SHULL, *Langmuir* **17** (2001) 4948.
21. A. J. CROSBY, K. R. SHULL, Y. Y. LIN and C. Y. HUI, *J. Rheol.* **46** (2002) 273.
22. K. L. JOHNSON, K. KENDALL and A. D. ROBERTS, *Proc. R. Soc. Lond.* A **324** (1971) 301.
23. HERTZ, "Miscellaneous Papers" (Macmillan, London, 1896).
24. A. J. CROSBY, A. KARIM and E. J. AMIS, *J. Polym. Sci. Pt. B-Polym. Phys.* **41** (2003) 883.
25. J. C. MEREDITH, A. KARIM and E. J. AMIS, *Macromolecules* **33** (2000) 5760.
26. *Idem.*, *MRS Bulletin* (2002) 330.
27. C. Y. HUI, Y. Y. LIN, J. M. BANEY and E. J. KRAMER, *J. Polym. Sci. Pt. B-Polym. Phys.* **39** (2001) 1195.
28. M. K. CHAUDHURY and G. M. WHITESIDES, *Langmuir* **7** (1991) 1013.
29. D. AHN and K. R. SHULL, *Macromolecules* **29** (1996) 4381.
30. R. DANZEBRINK and M. A. AEGERTER, *Thin Solid Films* **351** (1999) 115.
31. R. GRUNWALD, H. MISCHKE and W. REHAK, *Appl. Opt.* **38** (1999) 4117.
32. Y. LU, Y. YIN and Y. XIA, *Adv. Mater.* **13** (2001) 34.
33. T. OKAMOTO, M. MORI, T. KARASAWA, S. HAYAKAWA, I. SEO and H. SATO, *Appl. Opt.* **38** (1999) 2991.
34. Q. J. PENG, Y. K. GUO and S. J. LIU, *Opt. Lett.* **27** (2002) 1720.
35. S. HASELBECK, H. SCHREIBER, J. SCHWIDER, N. STREIBL, *Opt. Engin.* **32** (1993) 1322.
36. M. Y. M. CHIANG, W.-L. WU, J. HE and E. J. AMIS, *Thin Solid Films* **437** (2003) 197.
37. R. SONG, M. CHIANG, W.-L. WU and A. KARIM, *Unpublished Results* (2002).
38. S. ROBERSON, A. SEHGAL, A. FAHEY and A. KARIM, *Appl. Surf. Sci.* **203** (2003) 855.
39. R. SONG, A. J. CROSBY and A. KARIM, *Unpublished Results* (2002).